J Am Oil Chem Soc (2014) 91:885–903
DOI 10.1007/s11746-014-2435-0

ORIGINAL PAPER

Structure and Physical Properties of Plant Wax Crystal Networks and Their Relationship to Oil Binding Capacity

Alexia I. Blake · Edmund D. Co · Alejandro G. Marangoni

Received: 22 July 2013 / Revised: 19 January 2014 / Accepted: 3 February 2014 / Published online: 16 February 2014

Abstract The microstructure, melting and crystallization behavior, rheological properties and oil binding capacity of crystalline networks of plant-derived waxes in edible oil were studied and then compared amongst different wax types. The critical concentrations for oleogelation of canola oil by rice bran wax (RBX), sunflower wax, candelilla wax, and carnauba wax were 1, 1, 2, and 4 %, respectively, suggesting RBX and sunflower wax are more efficient structurants. A phenomenological two-phase exponential decay model was implemented to quantify the oil-binding capacity of these oleogels. Parameters obtained from this empirical model were then evaluated against microscale structural attributes such as crystal size, mass distribution and porosity to determine the structural dependence of oil-binding capacity. Gels containing candelilla wax exhibited the greatest oil-binding capacity, as they retained nearly 90 % of their oil. This is due to the small crystal size as well as the spatial distribution of these crystals. Using a microscopic to macroscopic approach, this study examines how the structural characteristics unique to each wax and resulting oleogel system affect functionality and macroscopic behavior.

Keywords Oleogel · Wax · Network · Microstructure · Oil binding

A. I. Blake · E. D. Co · A. G. Marangoni (✉)
Department of Food Science, University of Guelph, Guelph, ON, Canada
e-mail: amarango@uoguelph.ca

Introduction

The negative health effects of *trans* and saturated fatty acids on human health has been the subject of intense discussion for several decades. Numerous studies have shown that excessive intake of such dietary components, particularly *trans* fatty acids, can increase the risk of cardiovascular disease by lowering serum levels of high density lipoprotein while increasing the serum concentration of low density lipoprotein. A high dietary intake of saturated and *trans* fatty acids has also been correlated to an increased risk of other diseases such as coronary heart disease, Type II diabetes, obesity, stroke, metabolic syndrome and other cholesterol maladies [1].

For these reasons, the American Heart Association recommends that individuals do not consume more than 2 g of *trans* fats daily, which is equivalent to 1 % of the average daily caloric intake [2]. Governments have also passed legislation limiting the amounts of *trans* fatty acids that can be present in commercial food products. In some cases, governments go so far as to institute a total ban on *trans* fatty acids from foods. In 2003, Denmark was the first country to limit the amount of *trans* fatty acids in commercial food products to 2 % of the daily caloric intake, followed by Switzerland in 2008 [3]. The Canadian and American governments have yet to pass such regulations although *trans* and saturated fat labelling is mandatory by law [4].

Saturated and *trans* fatty acid levels can be particularly high in margarines, shortenings, and frying fats as well as foods consisting predominantly of lipids. Fat products are structured by triacylglycerols (TAG) containing high-melting fatty acids such as saturated and *trans* fatty acids. At the microstructural level, solid fats consist of a continuous three-dimensional network of aggregated clusters

of TAG crystals. TAG crystals are formed during a liquid to solid state transition when the fat is cooled from the molten state [5]. These same TAG molecules can pack into crystallographically different spatial arrangements in a phenomenon known as polymorphism. Polymorphism has a significant impact on the functionality of the resulting fat. For example, the β' polymorph present in margarine is responsible for its smooth texture and spreadability [6]. Alternatively, cocoa butter in chocolate products is tempered into the β_V polymorph to provide desirable sensory properties while avoiding bloom formation [7].

The structure of fats, as provided by the high-melting character of the constituent fatty acids, is responsible for the fat's functionality, sensory and textural attributes [8]. As well, a high degree of saturation results in a fat that is more stable towards oxidative degradation. Functional fat products used at an industrial scale are commonly obtained via the partial hydrogenation of liquid vegetable oils. The elimination or reduction of saturated and *trans* fatty acids from food products represents a conundrum to the food manufacturer. While reducing the levels of such fatty acids will result in a healthier food product, the textural quality of the food product will be negatively affected. Removal of saturated and *trans* fatty acids thus necessitates the development of a material which can serve as an alternative to fats in terms of functionality.

Finding such "alternative fats" has proven to be challenging. One of the approaches commonly investigated to create a fat-like substance is the gelation of liquid edible oils by an organogelator. Such a material behaves like a solid fat despite containing high amounts of unsaturated fatty acids. The triacylglycerols containing these fatty acids are commonly in the liquid state at ambient temperatures and so do not directly contribute to the texturing of the material.

The definition of a gel has proven to be a difficult task. Various definitions, many controversial and not widely-accepted, have been suggested over the years. Perhaps the most commonly cited definition is that proposed by Flory, which states that a material is a gel if it meets two requirements. First, the substance must have a continuous microscopic structure with macroscopic dimensions that are permanent on the time scale of an analytical experiment. Secondly, the substance must exhibit solid-like rheological behavior despite its high liquid volume fraction [9].

Structuring of liquid oil into a gel-like material can be achieved through many means. One such means involves the development of networks of colloidal crystalline particles such as those formed by the crystallization of triacylglycerols, diacylglycerols, monoacylglycerols and fatty acids [10]. The size, shape, and distribution of these crystals, as well as intercrystalline interactions all contribute to the mechanical properties of the resulting network which structures the liquid component of the system. Other structurants include gelators such as low molecular weight organogelators, which can self-assemble into fibrillar networks. These gelators, such as 12-hydroxystearic acid, are known to form helical and twisted ribbons that are hundreds of micrometers in length. These ribbons can form networks that entrap the liquid oil phase.

Plant wax esters are one class of organogelators that have been shown to successfully gel liquid oil. Their appeal is not only in that such materials are widely available, but also in that they are efficient, i.e., able to form gels at low concentrations ranging between 1 and 4 % (w/w). Previous studies have shown that the chemical nature of the type of wax affects the network characteristics of the gel. The gelation mechanism is attributed to the arrangement of *n*-alkanes or wax esters into small microcrystalline platelets, which, upon aggregation, form a complex three-dimensional network that easily entraps liquid oil.

A class of substances that shows great promise in creating fat-like materials is plant wax. The feasibility of a number of plant waxes as organogelators have been extensively studied. The studied waxes are some of the major plant waxes (in terms of both use and availability) and include rice bran wax (RBX) [11], candelilla wax [12], carnauba wax [14], sunflower wax [13] and more recently, sugarcane wax [14].

While no numbers for the annual worldwide production of RBX is available, the total potential of RBX can be estimated from the production of associated products such as rice and rice bran. The annual rice production in 2012 was estimated to be 731 million metric tons [15]. Of these, assuming that bran constitutes 8 % of the rice kernel [16], global rice bran potential can be estimated at 58 million metric tons. Bran can be assumed to contain anywhere between 15 and 20 % oil and as such, a conservative estimate of the global rice bran oil potential is $\sim$9 million metric tons. Rice bran oil may contain anywhere between 0.4 and 1.5 % wax. A conservative estimate of the annual RBX potential is 35,100 metric tons.

Sunflower wax is a by-product of sunflower oil processing. As with RBX, the annual worldwide potential for sunflower wax is not available but can be estimated from the production of sunflower oil. The annual refined sunflower oil production for the year 2008–2009 was estimated to be 11.7 million metric tons [17]. Assuming a refining loss of 3.5 %, the annual crude sunflower oil production can be calculated to be 12.1 million metric tons. As crude sunflower oil typically contains 0.35–1.0 % wax [18], a conservative estimate of the annual sunflower wax potential is 42,300 metric tons.

Mexico is the sole producer of candelilla wax. The amount of candelilla wax produced in 2009 is relatively low amount—1,071 metric tons [19]. This is due to the prevalence of cheaper synthetic mineral waxes, which have been used successfully to replace candelilla wax in many applications. The annual world production of carnauba wax in 2006 is 22,409 tons. As such, RBX and sunflower wax are the waxes with the greatest potential as alternative oil-structuring agents given the relatively large annual production of these substances.

Plant waxes (as well as most other biological waxes) can structure liquid oil at very low concentrations into an edible oil organogel, otherwise known as an oleogel. Plant waxes can effectively gel liquid oil at wax concentrations as low as 1–4 % (w/w). This attribute, coupled with the fact that plant waxes are readily available (as they are often by-products of agricultural and industrial processes) and are safe for consumption, makes them an economically feasible oil structurant. To date, plant waxes are already used in many commercial products, including cosmetics, lubricants, pharmaceuticals and coatings.

However, as the use of these waxes as oil-binding materials is a relatively new concept, an understanding of the gelation mechanism and the physical properties of such systems is lacking. Work carried out by Toro-Vazquez et al. [12] and Dassanayake et al. [11, 20] has provided insight into the fundamental physical characteristics of candelilla wax and RBX. Waxes are chemically diverse substances. Waxes can contain numerous chemical classes such as wax esters, hydrocarbons, alcohols, phenolic esters, to name a few. This chemical diversity complicates an accurate characterization of the structure and properties of plant waxes, as the presence of impurities significantly influence the gelation of these waxes, as was recently discussed by Hwang et al. [13]. For these reasons, comparative studies on the structure and properties of plant waxes are necessary.

This study uses a microscopic to macroscopic approach to determine how the molecular nature and microstructural properties such as crystal size and mass distribution, unique to each wax type, affect bulk scale properties and gel functionality such as the mechanical properties and oil-binding capacity of the resulting gel. It is reasoned that conditions that lead to the formation of small wax crystals (such as a high cooling rate) will result in a material with high G′ and yield stress as well as a higher oil-binding capacity. Similarly, large wax crystals (such as those formed under a low cooling rate) will result in a material with a low G′ and yield stress as well as a lower oil-binding capacity.

Table 1 Chemical composition of the plant waxes used in this study

Material	RBX	SFX	CLX	CRX
Ester content (%)	92–97	97–100	27–35	84–85
Free fatty acid (%)	0–2	0–1	7–10	3–3.5
Free fatty alcohol (%)	–	–	10–15	2–3
Hydrocarbons (%)	–	–	50–65	1.5–3
Resins/others (%)	3–8	0–3	–	6.5–10
Melting point (°C)	78–82	74–77	60–73	80–85

Studied waxes include *RBX* rice bran wax, *SFX* sunflower wax, *CLX* candelilla wax, *CRX* carnauba wax

Materials and Methods

Materials

The composition of RBX, sunflower wax (SFX), candelilla wax (CLX), and carnauba wax (CRX) were obtained using the technical brochures of the manufacturer (Koster Keunen Inc., Connecticut, USA). The chemical composition of the waxes is shown in Table 1.

Sample Preparation

Oleogels were prepared by mixing the appropriate wax with canola oil and then heating the mixture to 90 °C in a convection oven. The mixture was heated for 30 min to completely dissolve the waxes, after which time, the mixture was deposited onto a receptacle appropriate for the analysis (glass slides, X-ray slides, DSC pans, etc.). The gel was allowed to cool quiescently at ambient temperatures between 23 and 25 °C for at least 24 h before subjecting it to further testing. Testing was conducted on triplicate sample sets, with all gel concentrations reported as percentages (% w/w). Most of the analyses were conducted on organogels at the critical concentration, which is the minimum concentration of wax gelator necessary to form a self-standing gel.

Brightfield Microscopy

The concentrations of the organogel samples analyzed using brightfield microscopy were the respective critical concentrations of each wax type. Samples were prepared by depositing a drop of the molten gel onto a heated glass microscope slide. The molten gel was pressed with a preheated glass cover slip to ensure a sample thin enough for light microscopy. Slides were allowed to cool to ambient temperatures and remain at this temperature for at least 24 h before imaging. Imaging was likewise conducted at ambient temperatures. The microscope used to image the

gels was an Olympus BH light microscope operating in a standard brightfield configuration.

Fractal Dimensions and Porosity

The box-counting fractal dimension of the micrographs of each organogel at the critical concentration was determined using Benoit 1.3 (Trusoft International Inc, St. Petersburg, FL, USA). Micrographs were thresholded using Adobe Photoshop CS2 (Adobe Systems Inc, San Jose, USA) using the automatic threshold setting. Thresholded images were then processed by Benoit 1.3 to give a fractal dimension. The reported fractal dimension is an average taken from three micrographs. The porosity is a related measurement which can be calculated from the amount of white pixels (representative of the crystalline matter) in each micrograph. The amount of white pixels is reported as the % Fill, which is the percentage of white pixels out of all the pixels in the micrograph. The porosity, as calculated from the % Fill is calculated as:

$$\text{Porosity} = \left(1 - \frac{\%\text{Fill}}{100}\right) \quad (1)$$

Powder X-ray Diffraction

Samples (neat/bulk waxes 10 and 20 % organogels) for powder X-ray diffraction were prepared by filling the well of a glass sample holder with the molten solution until the well was level with the surrounding slide. The slides were cooled to ambient temperature and allowed to remain at this temperature for at least 24 h before analysis. The diffraction patterns were obtained using a Rigaku Multiflex X-ray diffractometer (Cu source with $\lambda = 1.5459$ Å). Wide angle X-ray scans (2θ range 1.2°–35° at 1.2°/min) and small angle X-ray scans (2θ range 1°–5° at 0.1°/min) were performed at ambient temperature and collected in triplicate.

Differential Scanning Calorimetry

The melting and crystallization behavior of the wax gels was studied using a TA Instruments Q2000 Differential Scanning Calorimeter. The samples for DSC measurements were prepared by placing a weighed amount of the molten gel (3–7 mg) in an aluminum pan. The pans were then hermetically sealed and stored at ambient temperature for at least 24 h prior to testing. DSC samples containing 1–5 % wax (w/w), as well as 10–90 % (w/w) wax were studied.

The thermal regimen employed in the test was as follows: heating from an initial temperature of 20–90 °C at a rate of 5 °C/min, followed by cooling from 90 to 20 °C at the same rate.

The peak melting temperatures (T_m), peak crystallization temperatures (T_c), enthalpy of melting (ΔH_m) and enthalpy of crystallization (ΔH_c) were determined from the DSC curves using TA Instruments' Universal Analysis Software supplied with the instrument. Results were obtained in triplicate.

Critical Concentration

The critical concentration, denoted as C^*, is defined in this study as the minimum amount of solid wax necessary to gel liquid oil. This was determined by formulating mixtures with increasing concentrations of waxes in a series of cylindrical 20-mL scintillation vials. The vials were filled halfway through with approximately 10 mL of the molten wax organogel preparation. The molten wax organogel preparation was allowed to cool to ambient temperatures prior to testing and was likewise tested at these temperatures. Testing was achieved via inversion of the containers. The concentration at which there is no visually-observable flow within the vial was taken to be the C^*.

Small Angle Controlled Stress Dynamic Rheology

The storage modulus (G') and yield stress of the wax oleogels at their respective critical concentrations was determined via a stress sweep using a TA Instruments AR2000 Controlled Stress Rheometer. The yield stress was taken to be the stress at which the G' exited the linear viscoelastic region. The G' and the yield stress were obtained under isothermal (20 °C) conditions at a constant frequency of 1 Hz using a steel 40-mm 2° cone and plate geometry. Results were obtained in triplicate using samples stored at ambient temperature for 24 h.

Pulsed Nuclear Magnetic Resonance

Using a Bruker PC/20 Series Minispec NMR Analyzer, the solids content of the wax oleogels was obtained for gels containing 1–90 % (w/w) wax, as well as for neat waxes. The measurements were obtained in triplicate at 25 °C.

Oil Binding Capacity

Oil-binding measurements were obtained using an in-house method. Glass funnels (8 cm diameter) were secured to test tube stands and lined with Whatman # 5 filter paper (125 mm diameter). One hundred grams of the organogel sample (with concentrations at the critical concentration) was spooned onto the funnel lined with filter paper. The organogel was not formed into a shape prior to introduction

to the funnel. The funnel was positioned above a beaker into which the oil from the gel dripped. The amount of oil in the beaker was measured at the following time intervals: 0.25, 0.5, 0.75, 1, 1.5, 2, 3, 4, 5, 6, and 24 h. Testing was conducted at 40 °C. The measurements were performed in triplicate.

Statistical Analysis

GraphPad Prism 5.0 (GraphPad Software, San Diego, CA, USA) was used for all data manipulation, curve-fitting and statistical analysis. Linear correlations analysis between the microstructural data and oil-binding parameters of the four gels at critical concentration were conducted. There were three replicates for each measurement for each gel. The level of significance for a correlation was arbitrarily chosen as $p < 0.20$ due to offset the low number of points available for the correlation.

Results and Discussion

The critical concentration (C^*) was 1 % (w/w) for both RBX and SFX, 2 % (w/w) for CLX and 4 % (w/w) for CRX. These findings are in accordance with those reported previously [11, 12, 20]. These findings suggest that waxes are relatively very efficient structuring agents in the sense that only a very small amount of wax is needed to structure large quantities of oil.

From the NMR results, it can be noted that the bulk/neat waxes do contain some minor liquid components, likely classified as resins/others. The solids content (in % mass/mass) for neat RBX, SFX, CLX, and CRX was determined to be 93.05 % ± 0.02, 97.8 % ± 0.05, 99.1 % ± 0.06 and 98.7 % ± 0.12, respectively. Using these values, a theoretical solid fat content (SFC) for gels containing varying concentrations of wax can be determined, assuming ideal solubility (Table 2). The theoretical solids content can be calculated by multiplying the percentage of the wax added to the organogel preparation (as formulated in the laboratory) by the measured solids content of the neat wax preparation as provided above. These theoretical values are slightly higher than experimental values obtained using NMR, perhaps suggesting slight wax solubility in liquid oil. This is in conjunction with the observation that a gelator must neither be too soluble nor insoluble in a solvent in order to achieve a proper balance of gelator–gelator interactions and gelator–solvent interactions. If the gelator is too insoluble, it will precipitate out of the solvent. Alternatively, if the gelator is too soluble in the solvent, i.e., interacts strongly with the solvent, a gel network will not be formed efficiently [21]. As observed in the critical concentrations of the wax gelator, wax solubility in canola oil seems to follow the order of RBX < SFX < CLX < CRX, assuming that these waxes all form microstructural elements of identical size and shape. The higher the concentration of wax required to form a self-standing organogel is indicative of the solubility of the wax in the oil, all other things being equal (which they are obviously not, but let us assume they are for the moment). The reasoning is that the more soluble the wax is in the oil, the necessary critical concentration of wax is greater. Thus, RBX has the lowest solubility as it requires the least amount of added wax in order to form a self-standing gel. On the other hand, carnauba wax is the most soluble as a relatively high minimum concentration is required to form a self-standing gel.

It must also be noted in passing that the oil type exerts a considerable effect on the critical concentration of a gelator. Thus, the critical concentration will vary depending on the type of oil used in the formulation of the organogel. This may be attributed to differences in solubility of a certain gelator in different oils. As was discussed by Dassanayake et al. [20], the oil type can also affect the crystallization kinetics, viscosity, crystal dispersion and hardness of gels made with RBX. They attributed these mechanical changes to the fatty acid composition of the

Table 2 Comparison of mean expected and measured solid fat content (SFC, %) for wax gels in canola oil at 25 °C

Wax		SFC (%)					
		5 %	6 %	7 %	8 %	9 %	10 %
RBX	Theoretical	4.67	5.61	6.54	7.48	8.41	9.35
	Measured	3.64 ± 0.07	4.36 ± 0.02	5.04 ± 0.19	5.44 ± 0.05	6.01 ± 0.21	6.91 ± 0.18
SFX	Theoretical	4.89	5.87	6.85	7.20	8.8	9.78
	Measured	4.24 ± 0.18	4.87 ± 0.02	5.56 ± 0.07	6.54 ± 0.08	7.34 ± 0.09	8.36 ± 0.1
CLX	Theoretical	4.96	5.95	6.94	7.93	8.92	9.91
	Measured	4.1 ± 0.13	4.83 ± 0.14	5.8 ± 0.16	6.66 ± 0.01	7.52 ± 0.24	8.36 ± 0.15
CRX	Theoretical	4.94	5.92	6.91	7.90	8.89	9.87
	Measured	4.47 ± 0.34	5.51 ± 0.15	6.44 ± 0.05	7.47 ± 0.24	8.35 ± 0.05	9.18 ± 0.13

The difference between expected and measured SFC indicates the amount of soluble wax in a gel at a given wax concentration

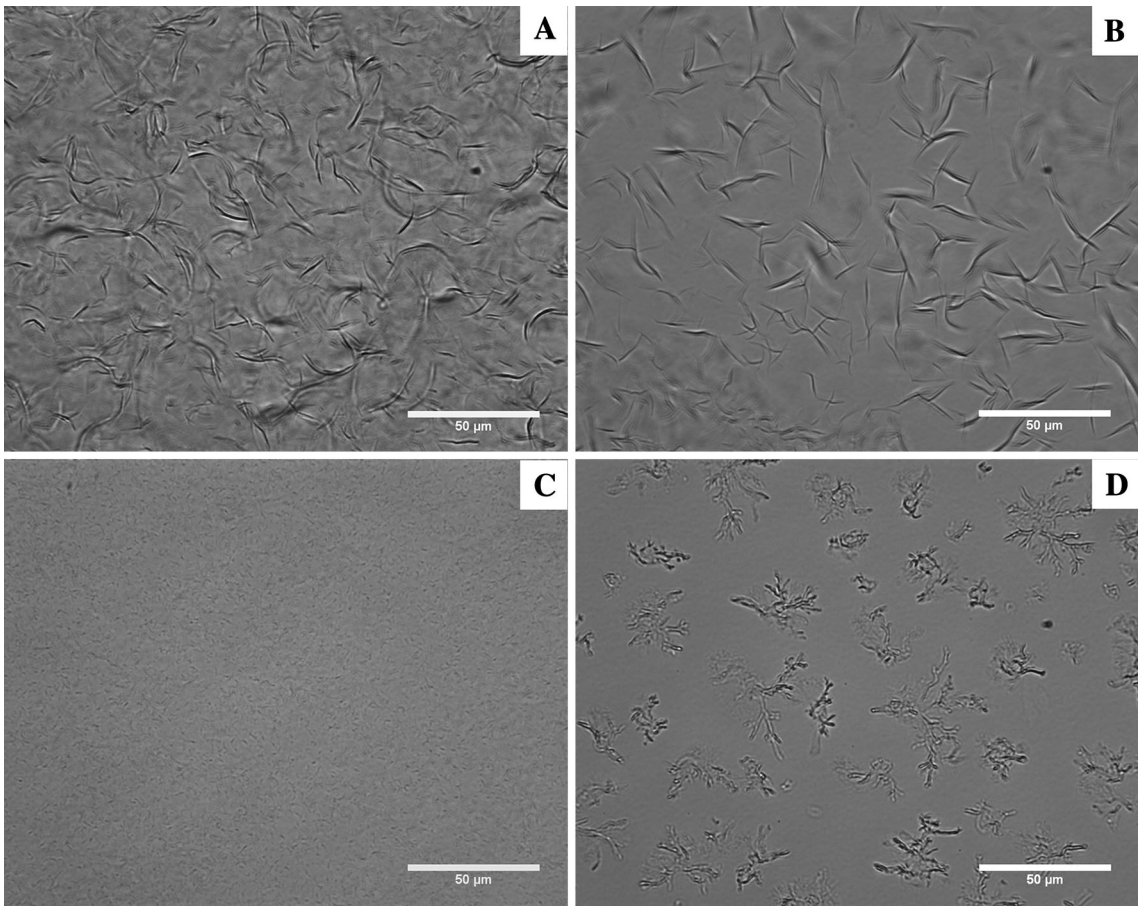

Fig. 1 Brightfield light micrographs of wax organogels consisting of canola oil and rice bran wax **(a)**, sunflower wax **(b)**, candelilla wax **(c)** and carnauba wax **(d)** at their respective critical concentrations

evaluated oils, noting that oils with saturated fatty acids and high melting fatty acids produced highly viscous and hard oleogels.

Microscopy

In agreement with what was previously reported by Dassanayake et al. [11] and Toro-Vazquez et al. [12], the morphology of RBX can be described as needle-like and fibrous, with the length of the crystals ranging between 10 and 20 µm. In comparison, CLX exhibited finely dispersed grain-like crystals ranging between 3 and 5 µm in length. CRX contained dendritic crystals as can be seen in Figs. 1 and 2. The CRX crystals had an approximate diameter between 10 and 20 µm. SFX also showed fibrous crystals which were much longer (15 and 25 µm) than the fibrous crystals seen in the RBX sample. The differences in microstructure were so striking that microscopy could, in principle, be used to identify the actual type of wax. This is an important issue related to wax adulteration with other plant waxes. For example, by examining the microstructure, it would be extremely easy to detect the adulteration of Candelilla or Carnauba wax with the cheaper RBX.

The fibrous morphology characteristic of RBX is widely considered to be the reason why RBX is a highly efficient gelator capable of forming oleogels at the relatively low critical concentration of 1 % (w/w). A high aspect ratio morphology such as a fiber is considered ideal for gelation. This is because, for an equal amount of gelator mass, the surface area for a high-aspect ratio morphology (fiber) is much greater than for a lower aspect ratio morphology such as a sphere or a platelet. This high surface area allows for the formation of more contacts between the microstructural elements that are responsible for a gel's elastic and solid-like character, while also enabling greater interaction between the gelator molecules and the solvent. The fibrous morphology of SFX also explains its high gelation efficiency, i.e., low critical concentration.

It was also observed that crystal size increased with wax concentration as seen in Fig. 2. This is due to the increase in the amount of available crystalline material, making further crystal growth possible.

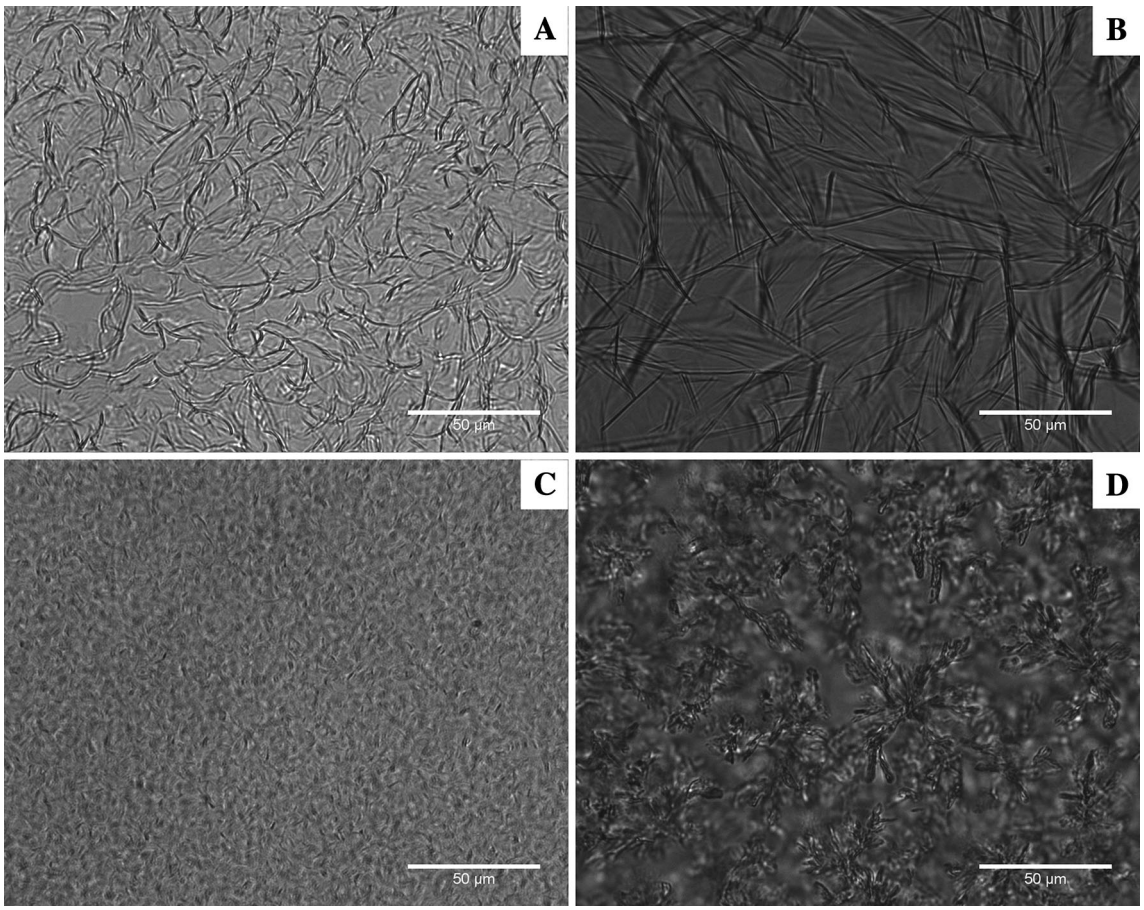

Fig. 2 Brightfield light micrographs of wax organogels consisting of canola oil and rice bran wax **(a)**, sunflower wax **(b)**, candelilla wax **(c)** and carnauba wax **(d)** at relatively high concentrations of 10 % w/w

Fractal Dimensions

A box-counting fractal dimension is an indicator of the spatial distribution of mass in a colloidal system, with greater fractal dimensions signifying more homogeneously distributed mass and/or more uniformly filled space, e.g., smaller or fewer pores. Although a comparative measure of mass dispersion could be qualitatively noted through visual observation of the thresholded micrographs (Fig. 3), numerical values allow for a more accurate description of mass distribution. As reported in Table 3, the fractal dimension increased in the following order: CRX < SFX < RBX < CLX. The significance of these results is further elaborated upon during the presentation and discussion of the oil-binding data.

Differential Scanning Calorimetry

The DSC thermographs of neat waxes exhibited single-peaks for RBX and SFX while showing multi-peak profiles for CLX and CRX (Fig. 4). Dilution shifted the melting endotherms to lower temperatures, depressing the melting point, and broadened the corresponding peaks (Fig. 5).

The peak melting temperatures (T_m) of the different organogels decreased in the order of CRX > RBX > SFX > CLX. The peak crystallization temperatures (T_c) of the various organogels decreased in the order of RBX > CRX > SFX > CLX (Fig. 5).

The peak melting temperature, peak crystallization temperature, enthalpy of melting (ΔH_m) and enthalpy of crystallization (ΔH_c) increased linearly with wax concentration, as seen in Figs. 6, 7 and 8, respectively. The enthalpy of melting and entropy of melting for neat wax and the gels at the critical concentrations are listed in Table 4.

It is important to consider the chemical nature and molecular composition of the waxes to properly understand the meaning of these thermodynamic results. As seen in Table 1, RBX and SFX are by far the most "chemically homogeneous" waxes, as their major components (>92 %) are wax esters. As they contain a single predominant chemical group, RBX and SFX melting and crystallization

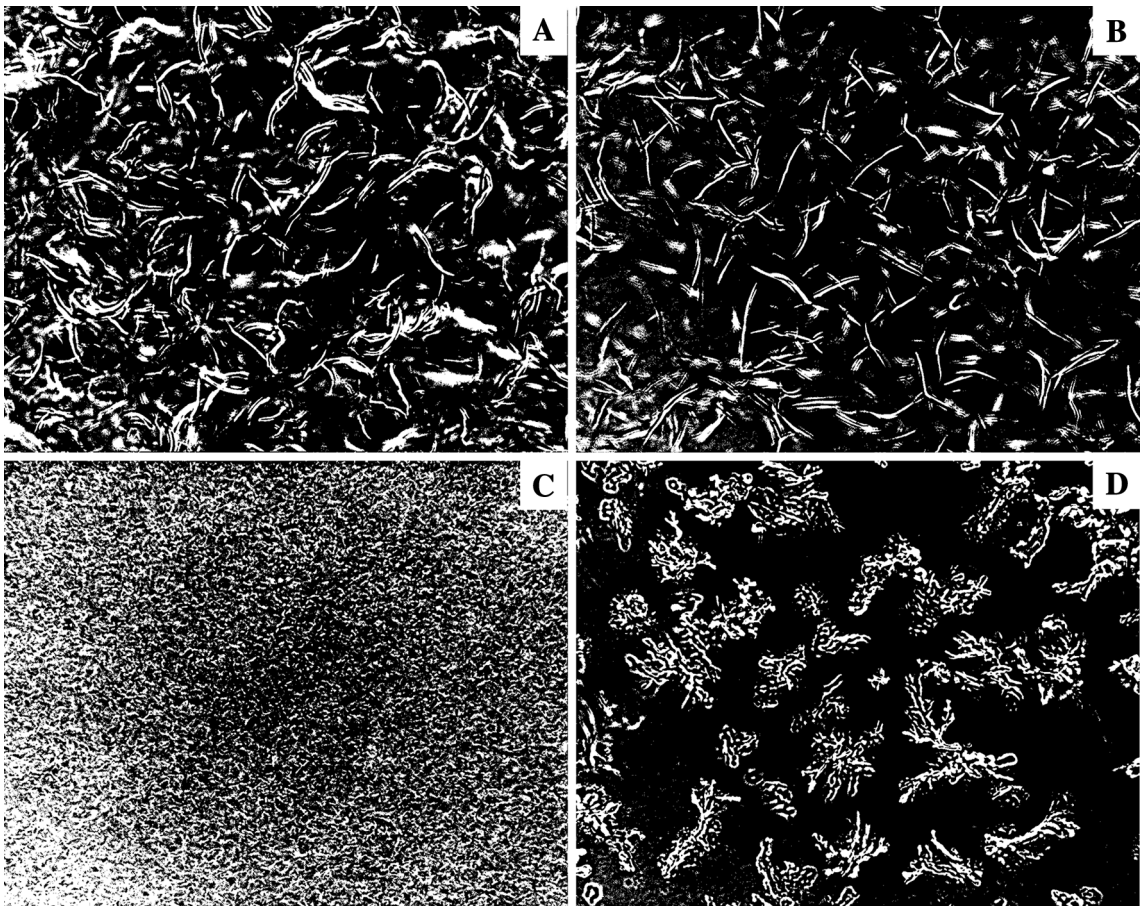

Fig. 3 Automatically thresholded brightfield light micrographs of wax organogels consisting of canola oil and rice bran wax **(a)**, sunflower wax **(b)**, candelilla wax **(c)** and carnauba wax **(d)** at their respective critical concentrations

Table 3 Box-counting fractal dimension (D_b) and porosity for the different waxes derived from brightfield micrographs of wax-oil gels at their respective critical concentrations

Sample	Box-counting fractal dimension (D_b)	Porosity
1 % Rice bran wax	$1.62^{a,b} \pm 0.1002$	$0.807^{a,c} \pm 0.005$
1 % Sunflower wax	$1.54^{a,b} \pm 0.1096$	$0.864^{a,b} \pm 0.022$
2 % Candelilla wax	$1.75^{a} \pm 0.1378$	$0.708^{c} \pm 0.058$
4 % Carnauba wax	$1.41^{b} \pm 0.0340$	$0.916^{b} \pm 0.047$

Means with the same superscript are not significantly different

transitions are characterized by narrow, single peaks. CLX and CRX differ significantly in this respect due to their heterogeneous chemical composition. For example, CLX is extracted from the external parts of *Euphorbia cerifera* and *Euphorbia antisyphilitica*, both native to north-western regions of Mexico and some south-western regions of Texas [22]. Toro-Vazquez et al. [12] have characterized the chemical composition of CLX as having high proportions of *n*-alkanes, with hentriacontane being the most prominent (78.9 %). Other alkanes, specifically nonacosane and tritriacontane, have been identified as minor components. With different melting and crystallization temperatures, this mixture of components will result in the observed double-peak endotherms and exotherms seen in CLX thermograms [18, 23]. Likewise, the presence of various chemical components with different thermal properties is responsible for the double-peak thermograph of CRX. This wax is obtained from the leaves of *Copernicia cerifera* C. Martius, a palm tree found in northeastern Brazil [22]. Depending on the maturity of the plant, four types of CRX can be extracted. The variability of CRX type as a function of plant age may explain its heterogeneous molecular composition. CRX contains 84 % esters, 6.5–9.5 % fatty acids, fatty alcohols, and hydrocarbons, and 6.5–10 % resins.

Previous studies have shown that the minor components in the waxes behave as impurities and affect crystallization kinetics due to structural compatibility (or lack thereof) and their own thermal behavior [24]. For example, the presence of minor components (such as diacylglyceols) in milk fat inhibits TAG crystallization. Wright and Marangoni [25] demonstrated that milk fat with diacylglycerol impurities

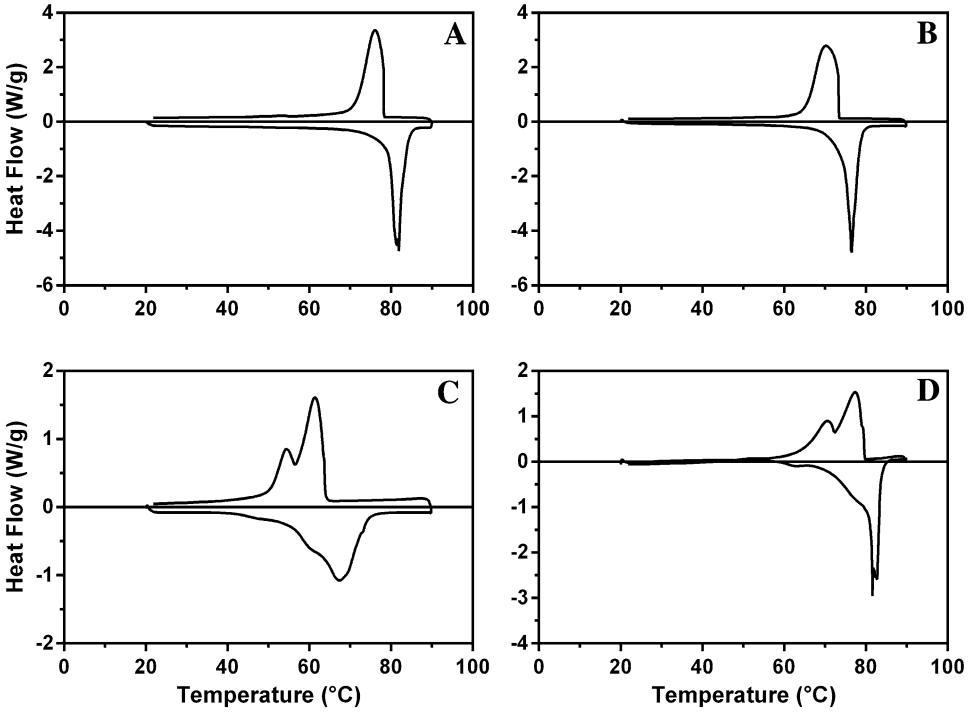

Fig. 4 Differential scanning calorimetric traces of the different *neat* waxes—rice bran wax (**a**), sunflower wax (**b**), candelilla wax (**c**) and carnauba wax (**d**) used in this study for both cooling (exotherms, positive heat flow) and heating (endotherms, negative heat flow) modes

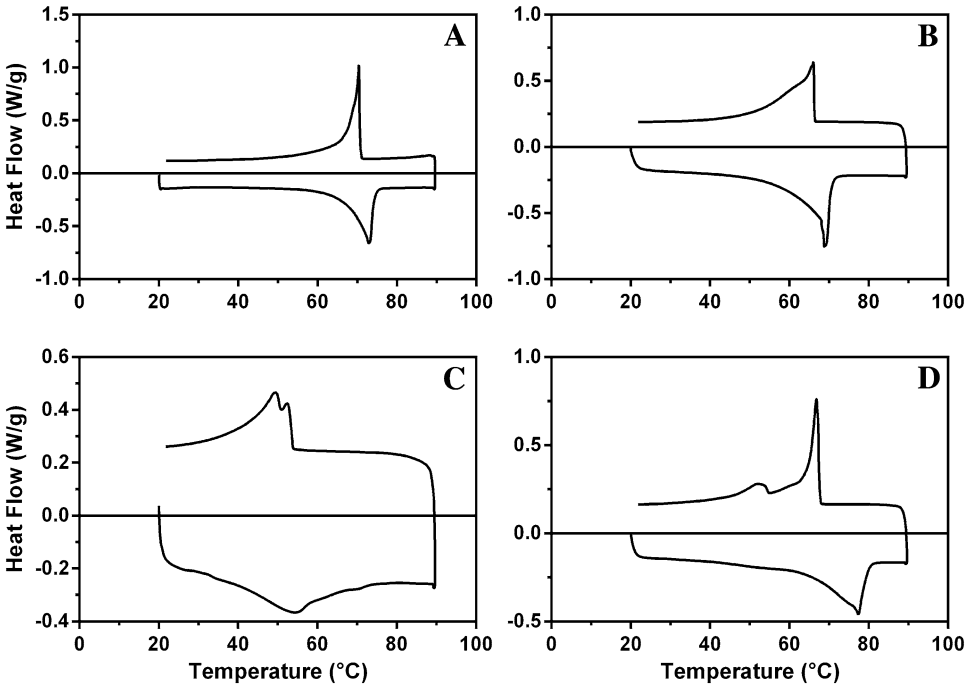

Fig. 5 Differential scanning calorimetric traces of the different wax organogels (in canola oil at concentrations of 20 % w/w)—rice bran wax (**a**), sunflower wax (**b**), candelilla wax (**c**) and carnauba wax (**d**) used in this study for both cooling (exotherms, positive heat flow) and heating (endotherms, negative heat flow) modes

needs to be undercooled by an additional 20 °C to initiate crystallization. Another common consequence of impurities are morphological changes, particularly with respect to crystal size [21]. With greater relevance to wax esters, a recent paper by Hwang et al. explored the gelation capabilities of plant and animal waxes in soybean oil. Their findings indicate that chemical purity, and more importantly, compatibility between many major and minor components, is required for good gelation properties. They also concluded wax esters with longer alkyl chains gel soybean oil more effectively, suggesting that waxes with longer chain wax esters will exhibit superior gelation compared to waxes with shorter chain wax esters [13].

SFX and RBX are known to have high ester contents. This, as well as their homogeneous chemical composition, appear once again to contribute to both their fibrous

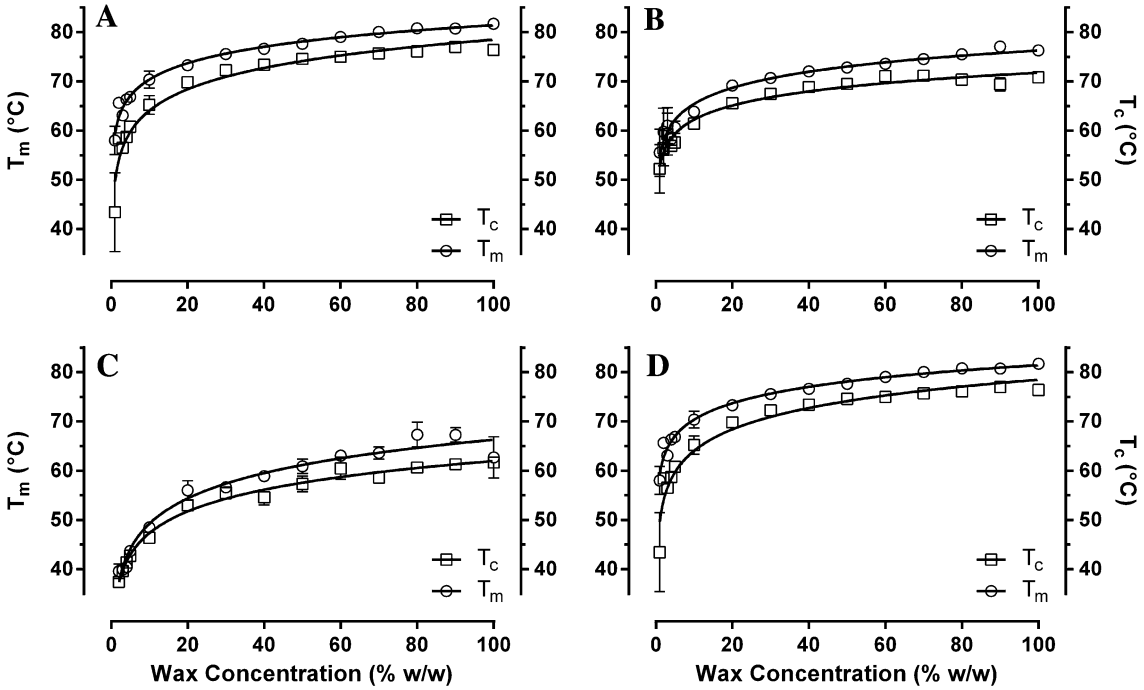

Fig. 6 Peak melting temperatures (T_m, ⊖) and peak crystallization temperatures (T_c, ⊟) as functions of the concentration of rice bran wax (**a**), sunflower wax (**b**), candelilla wax (**c**) and carnauba wax (**d**) in canola oil

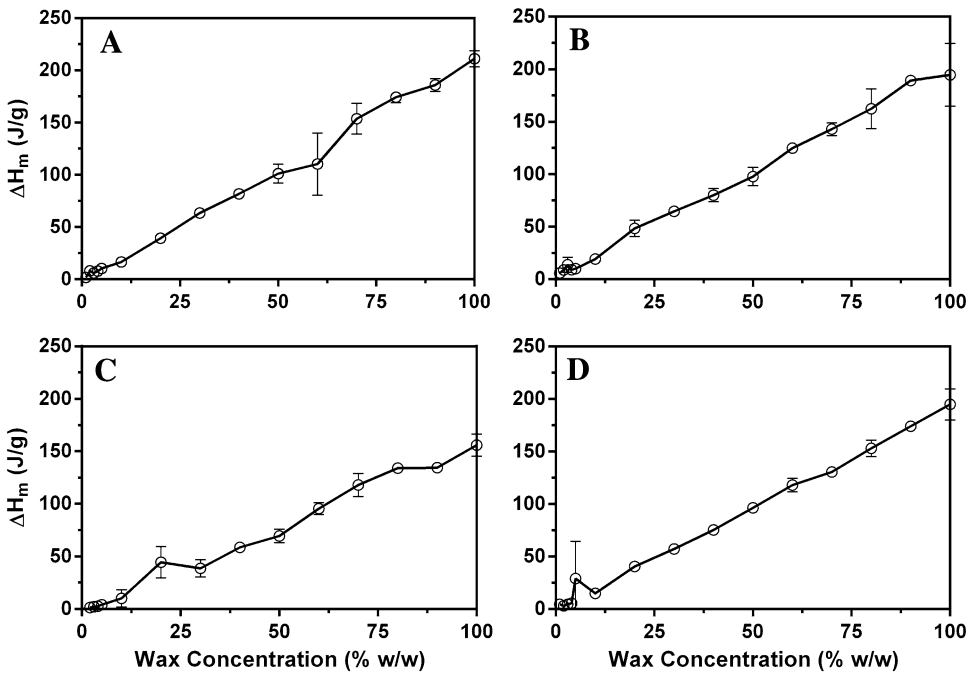

Fig. 7 Enthalpy of melting (ΔH_m) as a function of rice bran wax (**a**), sunflower wax (**b**), candelilla wax (**c**) and carnauba wax (**d**) concentration in canola oil

crystalline morphology, single peak exo- and endotherms, and their low critical concentration. For the same reason, the heterogeneous chemical composition of CLX and CRX result in crystallization behavior that results in a morphology markedly different from that of RBX and SFX. This is particularly evident in CLX, where the presence of minor components hinders crystal growth, resulting in a grain-like morphology, perhaps due to a lack of compatibility between major and minor components as discussed by Hwang et al. [13].

Toro-Vazquez et al. examined the effect of the heterogeneous composition of CLX in their study of the effects of tripalmitin crystallization on the thermomechanical properties of CLX organogels. The results, which included

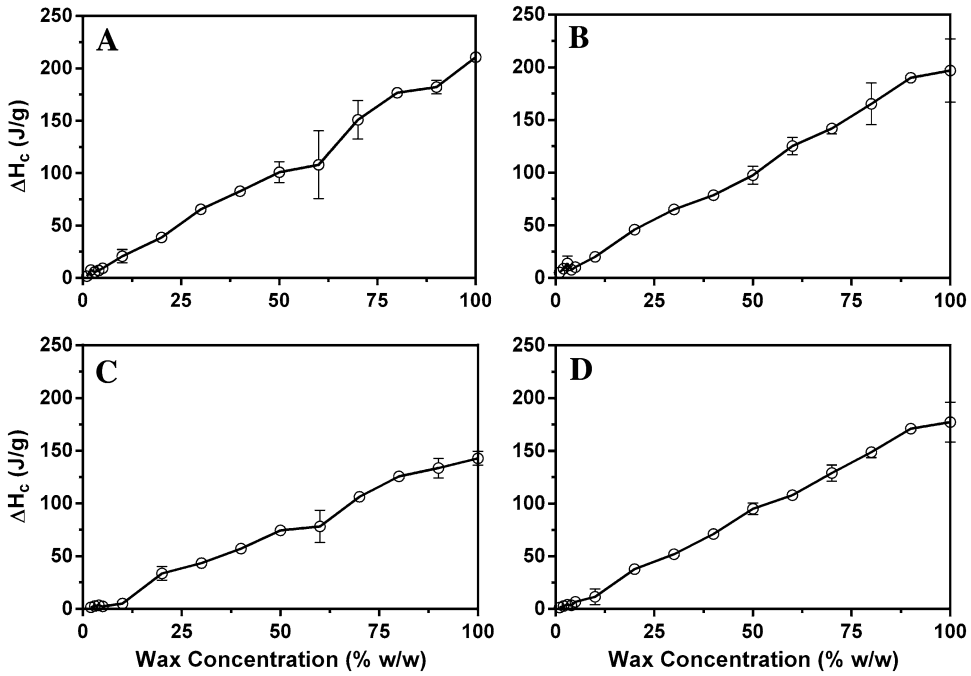

Fig. 8 Enthalpy of crystallization (ΔH_c) as a function of rice bran wax (**a**), sunflower wax (**b**), candelilla wax (**c**) and carnauba wax (**d**) concentration in canola oil

Table 4 Enthalpy and entropy of melting of rice bran wax (RBX), sunflower wax (SFX), candelilla wax (CLX) and carnauba wax (CRX) in the bulk state and in the gel state at the critical gelator concentration

	RBX		SFX		CLX		CRX	
	1 %	Neat	1 %	Neat	2 %	Neat	4 %	Neat
ΔH_m (J/g)	1.7 ± 0.53	211 ± 7.6	1.93 ± 0.30	195 ± 29.8	1.36 ± 0.84	156 ± 10.5	5.56 ± 0.21	195 ± 14.7
ΔS_m [mJ/(g K)]	5.13	595	5.87	557	4.36	464	15.8	553

increases in the number of crystals, storage modulus (G′) and yield stress (for 3 % CLX and 1 % tripalmitin compared to pure CLX gels), demonstrated that co-crystallization of TAG with CLX can be used to tailor the physiochemical properties of these oleogels [23]. Kerr et al. obtained similar results in their study on the effects of sunflower wax crystallization on anhydrous milk fat (AMF). Their findings showed that the addition of SFX to AMF modified its microstructure, texture, and melting profile [26].

The values for entropy of melting support these findings and the assumption regarding the role of minor components. Due to their greater chemical homogeneity, RBX wax esters crystallize into a more ordered solid state. This more ordered crystalline state should, and does, have a higher entropy of melting (ΔS_m) than that of CLX and CRX. On the other hand, CLX and CRX's heterogeneous chemical nature leads to the formation of mixed crystals upon crystallization. These mixed crystals are more disordered and thus should, and do have, a lower ΔS_m. Thus, we can conclude that CLX has the lowest ΔS_m due to a greater degree of crystalline disorder, and that this is due to its greater chemical heterogeneity.

X-Ray Diffraction

As previously reported by Dassanayake et al., wide angle diffraction scans for neat, 10 and 20 % gels indicated a β′, or orthorhombic, crystalline sub-cell arrangement for all waxes [11]. This particular polymorph is characterized by two wide angle peaks at 0.37 and 0.41 nm [7] (Fig. 9). Waxes had very similar wide angle diffraction patterns. Of note, the wide angle spacings for CLX deviated the most from expected literature values. This is perhaps due to the previously mentioned mixed molecular packing arrangement within CLX systems resulting from the presence of minor components.

RBX, SFX, and to a smaller extent, CLX, exhibited lamellar packing as can be evidenced by peaks in the SAXS region. There were no observable small angle peaks for CRX (Fig. 10). Note the large SAXS spacings for RBX and SFX. This is a direct consequence of their molecular composition, and is associated with their fibrous morphology.

It has been previously noted that the long-spacing patterns are significantly less intense than the short-spacing patterns. This is taken to indicate anisotropic

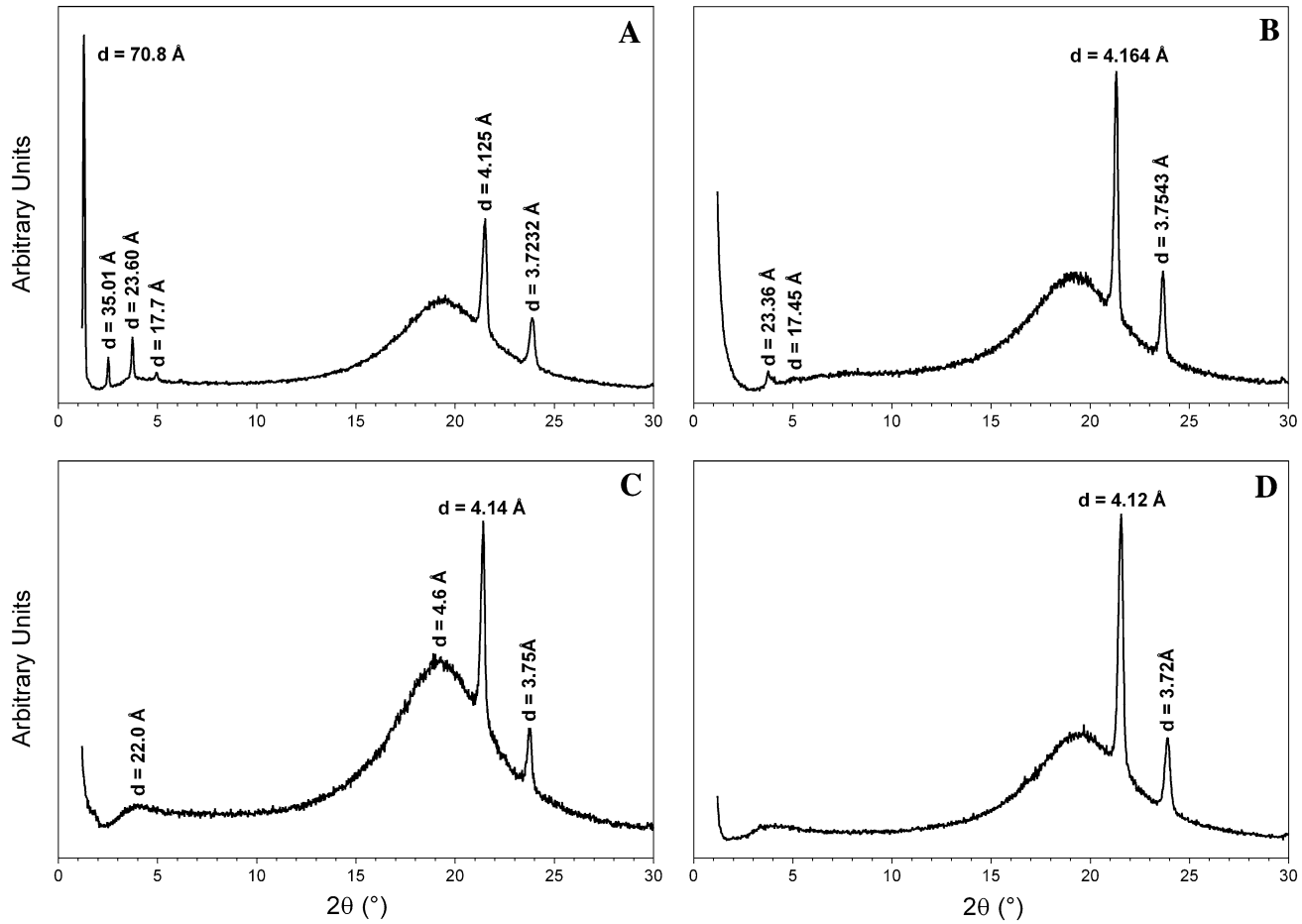

Fig. 9 Wide and small angle powder X-ray diffraction patterns for neat waxes—rice bran wax (**a**), sunflower wax (**b**), candelilla wax (**c**) and carnauba wax (**d**)

crystal growth along directions perpendicular and parallel to the lamellar planes [6]. Such growth is a consequence of strong van der Waal interactions between long hydrocarbon chains and polar (ester) functional groups between lamellar planes, resulting in high lateral growth rates [20]. Comparatively, the molecular interactions between terminal methyl groups is much weaker, leading to much slower growth in directions vertical (or perpendicular) to the lamellar plane.

Rheology

The elastic moduli (G′) and yield stresses of the wax organogels at their critical concentrations decreased in the order of CRX > CLX > RBX, SFX >1 % CLX, as can be appreciated in Fig. 11. It was observed that weak gels could be created containing 1 % CLX. However, these gels did not exhibit sufficient stability at temperatures >40 °C, for which reason 1 % cannot be taken as the critical concentration of CLX systems. Nevertheless, 1 % CLX gels were evaluated against other critical concentration samples in an effort to more accurately characterize these gels systems in their critical states. As an indicator of stiffness, the G′ for each type of organogel (Table 5) was significantly different between different types of gel ($p < 0.05$). Furthermore, G′ was shown to have a dependence on the wax concentration although this is hard to ascertain as the differences in G′ between very similar wax concentrations are well within the error of the instrument. At equivalent wax concentrations, the G′ for each type of wax organogel were also shown to be statistically different ($p < 0.05$), suggesting a contribution of each type of wax's unique structure to mechanical behavior.

The differences in the G′ of the various wax organogels can be attributed to microstructural factors such as the spatial distribution of mass (as given by the fractal dimension), the solids volume fraction and particle size. In general, the following trends can be observed between the G′ and the various microstructural factors mentioned. The G′ can be shown to increase with an increase in the solid volume fraction. The G′ also increases with a decrease in both the fractal dimension and the particle size [27, 28].

On the basis of solids volume fraction, CRX is understandably much harder than all the other wax organogels at

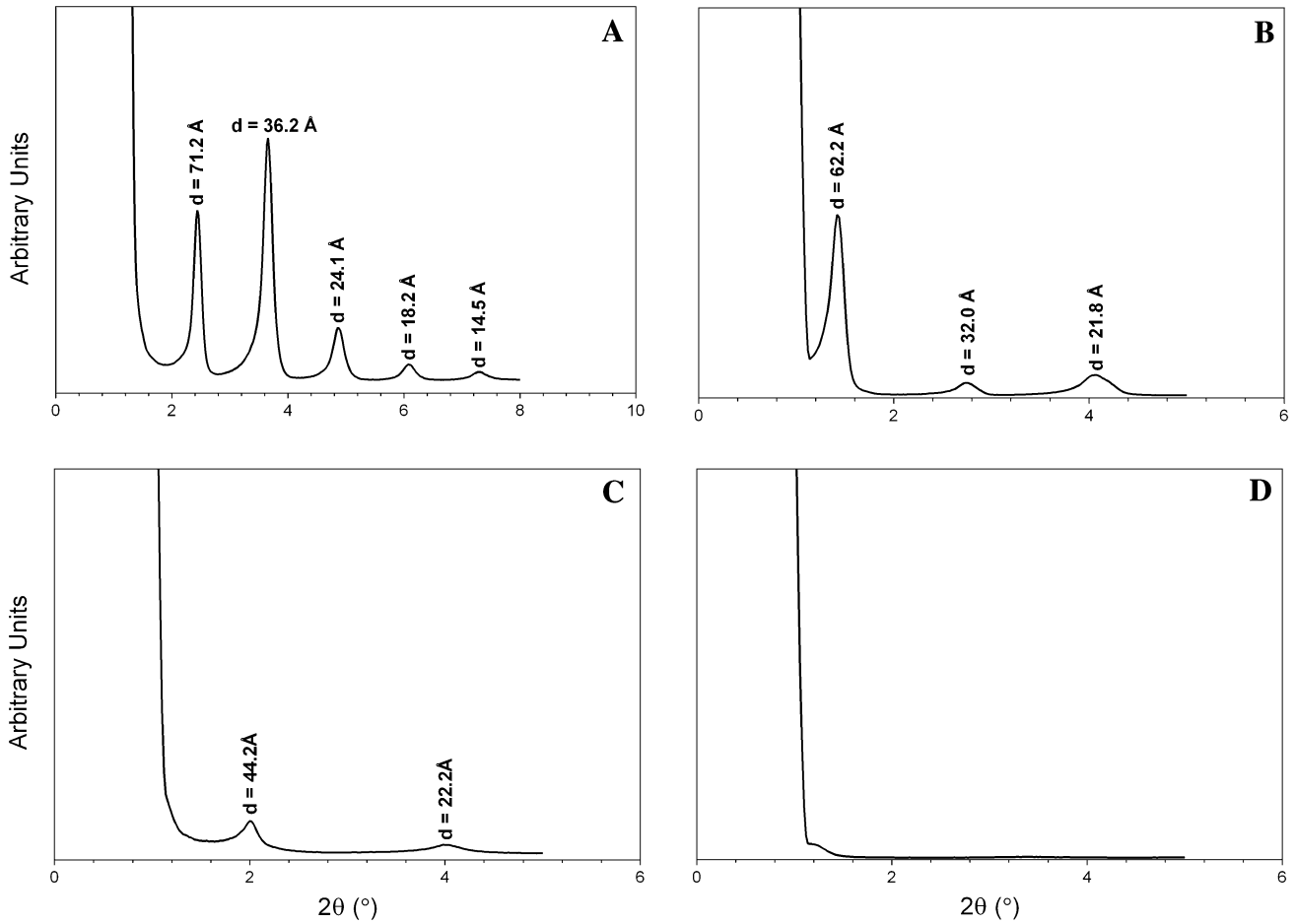

Fig. 10 Small angle powder X-ray diffraction patterns for neat waxes—rice bran wax (**a**), sunflower wax (**b**), candelilla wax (**c**) and carnauba wax (**d**)

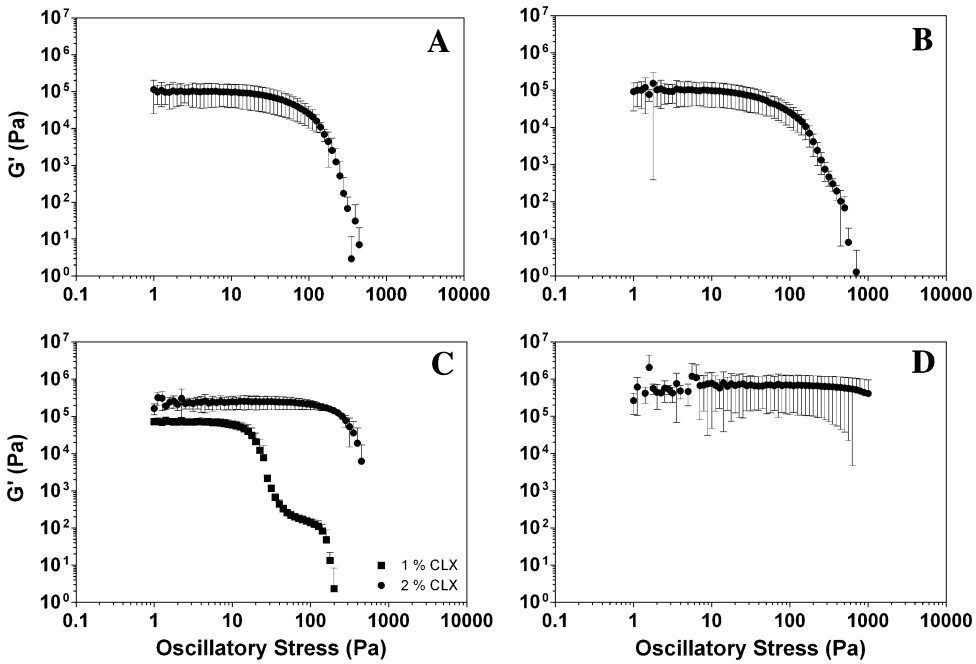

Fig. 11 Isothermal (20 °C) stress sweeps for wax organogels made with rice bran wax (**a**), sunflower wax (**b**), candelilla wax (**c**, *filled circles*) and carnauba wax (**d**) at the critical concentration as well as the 1 % w/w CLX gel (**c**, *filled squares*)

Table 5 Storage modulus, G′ (Pa), for various wax-canola oil oleogels containing varying amounts of rice bran wax (RBX), sunflower wax (SFX), candelilla wax (CLX) and carnauba wax (CRX)

% Wax	G′ (10^5 Pa)			
	RBX	SFX	CLX	CRX
Critical	1.01 ± 0.630	1.03 ± 0.677	2.28 ± 0.747	4.67 ± 2.76
5	0.164 ± 0.0491	0.0235 ± 0.0217	4.77 ± 1.04	1.84 ± 1.55
6	0.218 ± 0.0820	1.25 ± 0.665	6.19 ± 3.62	1.90 ± 1.49
7	4.88 ± 2.17	1.25 ± 1.38	9.78 ± 4.08	1.69 ± 4.21
8	11.9 ± 6.55	2.06 ± 0.985	3.19 ± 6.20	26.5 ± 4.50
9	8.30 ± 4.39	3.30 ± 1.99	30.9 ± 11.5	30.9 ± 11.5
10	5.05 ± 0.602	2.40 ± 2.03	16.8 ± 8.56	9.51 ± 6.88

the critical concentration considering that the minimum amount of solids needed to form a self-standing gel is much higher for CRX. The amount required is 4 % compared to 2 % for CLX and 1 % for either RBX or SFX. Likewise, CLX, at the critical concentration, is much harder than either RBX or SFX as the amount of wax solids added is at 2 %. Interestingly, the hardness of RBX and SFX are relatively similar, which is not unexpected in light of the similar wax concentrations added to these gels. The dependence of the G′ on the solids volume fractions exhibits a very good and predictable correlation.

On the basis of the fractal dimensions of the given organogels, one can arrange the G′ of the various organogels in the following decreasing order CRX > SFX > RBX > CLX. CRX can be seen to be much harder than the other three wax types, which is in agreement with the observed G′ results. However, the second hardest wax organogel, as predicted by the fractal dimension, is SFX, which is not the observed trend for the G′ values. The same observation can be made with RBX and CLX. The lack of agreement between the trends in the fractal dimension and the trends in the observed G′ can be attributed to differences in the particle morphology and particle size of the constituent microstructural elements of these wax organogels.

Examining the particle size of the microstructural elements of the wax organogels, one can see that CLX gels contain the smallest particles while the gels consisting of CLX, RBX and SFX have particles with similar dimensions. On this basis, CLX can be predicted to be much harder than either CLX, RBX or SFX. However, this is not the case.

The observed experimental trend for the hardness is a consequence of the interplay between all three microstructural factors. By virtue of the solids volume fraction, CRX is the hardest, followed by CLX and then by RBX and SFX. By virtue of the fractal dimension, CRX is the hardest, followed by SFX, RBX and then CLX. However, it can be reasoned that the contribution to hardness resulting from the small particle size of CLX allows it to be much harder than the gels made with SFX and RBX, hence its position as being the second hardest of the gels.

Oil-Binding Capacity

The amount of oil collected over a 24-h period, alternatively expressed as the amount of oil lost by a particular gel system, was used as an indicator of the oil binding capacity. The collected data obtained from this oil binding evaluation is in the form mass of oil lost in grams as a function of time in hours (Fig. 12). The data were fitted to a two-phase exponential decay model in the form of:

$$Y = Y_{\text{Fast}}\left(1 - e^{-k_{\text{fast}}t}\right) + Y_{\text{Slow}}\left(1 - e^{-k_{\text{slow}}t}\right)$$

$$Y_{\text{Fast}} = \Phi_{\text{Fast}} Y_{\max}$$

$$Y_{\text{Slow}} = (1 - \Phi_{\text{Fast}}) Y_{\max}$$

$$Y_{\max} = Y_{\text{Fast}} + Y_{\text{Slow}}$$

where t is time, Y_{Fast} is the amplitude of the fast-decaying component, Y_{Slow} is the amplitude of the slow-decaying component, k_{Fast} and k_{Slow} are the respective rate constants for each component. $Y_{\max}$ is the value of Y at sufficiently long (infinite) times and is the sum of both Y_{Fast} and Y_{Slow}. Φ_{Fast} is the fraction of $Y_{\max}$ that can be attributed to the fast-decaying component. Likewise, the difference $1 - \Phi_{\text{Fast}}$ is the fraction of $Y_{\max}$ that can be attributed to the slow-decaying component.

Oil-binding can examined from two different perspectives. From the first perspective, one can evaluate the oil-binding capacity of a material based on the maximum amount of oil that is expressed by the material over a specified (usually "long") length of time (in the case of this study, 24 h). This shall be called "long-term oil-binding". From the second perspective, one can evaluate the oil-binding capacity on the basis of the rate of oil loss, i.e., how quickly the material exudes oil, which shall be referred to as "short-term oil-binding". Naturally, the choice of an appropriate perspective is dependent on the

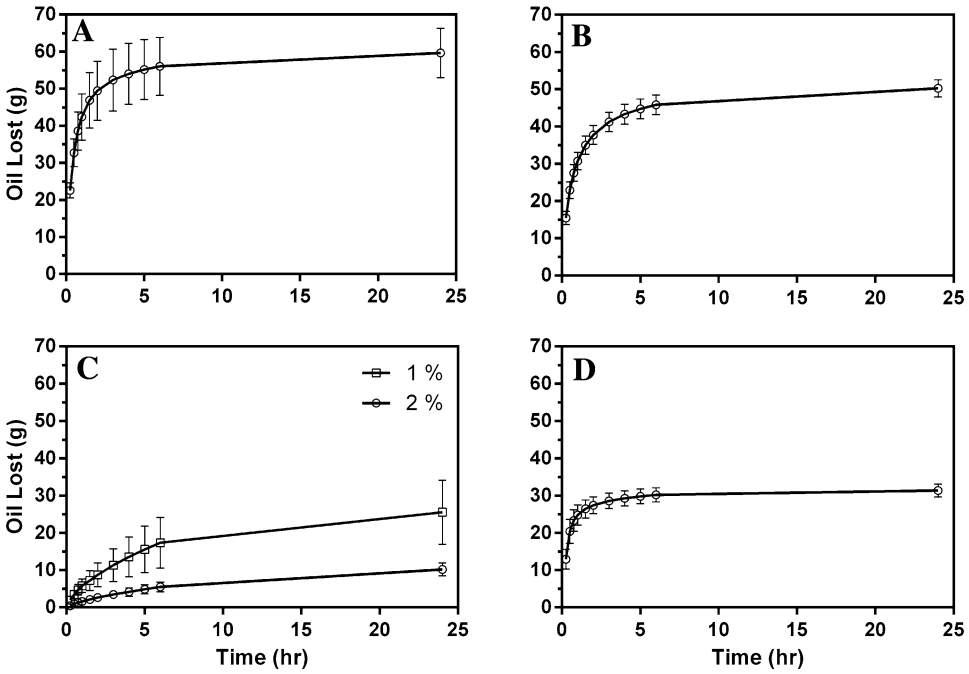

Fig. 12 Oil loss curves for organogels made with rice bran wax (RBX, *filled circles*), sunflower wax (SFX, *filled squares*), candelilla wax (CLX, *filled triangles*) and carnauba wax (CRX, *filled diamonds*) at the critical concentration as well as candelilla wax at the 1 % w/w concentration (CLX, *upside down filled triangles*)

circumstances of the analysis. The first perspective is appropriate in situations involving storage, where the long-term stability of a material is of interest. In this case, it would be desirable to have as little oil exude as possible even if the rate of oil exudation may be rapid. Likewise, the second perspective is appropriate in situations involving immediate use processing of the material after fabrication of the material. In this case, it would be desirable to have oil exude as slowly as possible to avoid complications in material handling and processing regardless of whether or not the quantity of oil that will eventually exude is large.

The model used in the analysis posits that the material in question contains two different species with regards to oil-binding capacity: a species that leaks oil relatively quickly (fast component) and a species that leaks oil relatively slowly (slow component), both of which can be differentiated based on the magnitude of the respective rate constants. As an interpretation, the fast component can be regarded as unbound (physically-entrapped) oil while the slow component can be regarded as bound oil, oil that is adsorbed on to the surface of the solid particles but is nevertheless released from the material. It is important to note that what defines "strongly-bound oil" is vague at best as strongly-bound oil can be interpreted as oil that is released slowly or oil that is not exuded at all over the time scale of the experiment. In this discussion, both oil that is exuded slowly and oil that is retained within the material throughout the length of the analysis shall be considered to be strongly-bound oil.

Thus, the analysis conducted allows a simultaneous examination of oil-binding from both long and short-term perspectives. The determined Y_{max} values (essentially the plateau value of the modeling function) gives an overall indication of the equilibrium amount of oil that will be lost from the material over lengthy periods of time. Likewise, the magnitudes of Y_{Fast} and Y_{Slow} are indicative of the time scale over which loss of stability mainly occurs. Y_{Fast} can also be interpreted as the percentage of the total amount of oil in the system that is weakly bound. The sum of Y_{Slow} and the percentage of oil that was not released is indicative of the percentage of the total amount of oil in the system that is strongly bound.

From examining the Y_{max} values (Table 6), it can be seen that the maximum amount of oil that is exuded by each gel increases in the order: 2 % CLX < 1 % CLX < 4 % CRX < 1 % SFX < 1 % RBX. Thus, gels made with candelilla wax will exude the least amount of oil over a long period of time. As well, the maximum amount of oil exuded decreases when the wax gelator concentration is increased as in the case of candelilla wax. From this, it can be concluded that candelilla wax has the strongest oil-binding capacity, followed by carnauba wax and then by sunflower wax with RBX having the least oil-binding capacity at their respective critical gelator concentrations.

An examination of the Y_{Fast} values (Table 6) of each gel shows that the Y_{Fast} values for the gels made with 1 % RBX, 1 % sunflower wax and 1 % candelilla wax are 20, 23 and 25 %, respectively. This indicates that roughly one-fifth to one-fourth of the total amount of oil in these gels is weakly bound. This suggests that roughly four–fifths to three-quarters of the oil in these gels are strongly bound. A similar examination of the Y_{Fast} values of the 2 % CLX and

Table 6 Fit parameters obtained by fitting the two-phase exponential decay kinetic model to the oil-binding data as discussed previously

	1 % RBX	1 % SFX	1 % CLX	2 % CLX	4 % CRX
Y_{max} (%)	59.34 ± 3.197	50.04 ± 1.162	25.98 ± 2.602	11.12 ± 1.202	31.36 ± 1.138
Y_{Fast} (%)	20.00 ± 7.835	23.20 ± 2.843	23.97 ± 3.489	10.33 ± 0.9171	7.066 ± 2.415
Y_{Slow} (%)	39.34 ± 8.474	26.84 ± 3.035	2.006 ± 3.230	0.7931 ± 1.302	24.30 ± 2.560
Φ_{Fast}	0.3370 ± 0.1334	0.4637 ± 0.05747	0.9228 ± 0.1223	0.9287 ± 0.1116	0.2253 ± 0.07659
$1 - \Phi_{Fast}$	0.6630 ± 0.1334	0.5363 ± 0.05747	0.0772 ± 0.1223	0.0713 ± 0.1116	0.7747 ± 0.07659
k_{fast} (h^{-1})	0.3294 ± 0.2224	0.3053 ± 0.06338	0.1665 ± 0.05806	0.1003 ± 0.04246	0.3006 ± 0.1886
k_{slow} (h^{-1})	2.872 ± 0.9665	2.670 ± 0.4647	3.095 ± 11.07	1.507 ± 3.497	3.017 ± 0.5473

4 % CRX, show that the Y_{Fast} values of these gels are 10 and 7 %, respectively. These results suggest that a smaller percentage of the total amount of oil in the 2 % CLX and 4 % CRX gels is weakly bound. It is interesting to note that as the amount of gelator is increased, the amount of oil that is weakly bound decreases, although this trend is hardly surprising.

An examination of the relative amounts of the Φ_{Fast} values (Table 6) shows that roughly 34, 46 and 23 % of the maximum amount of oil that is exuded, respectively, from gels made with RBX, sunflower wax and carnauba wax at their respective critical concentrations are fast-leaking. In contrast to this, the gels made with candelilla wax at concentrations of 1 and 2 %, show, respectively, that 92 and 93 % of the maximum oil exuded are fast-leaking. Thus, it can be concluded that the short-term stability of gels made with candelilla wax is poor given that most of the oil that is exuded is exuded relatively quickly, albeit the amount exuded is comparatively low. In a like manner, the short term stability of carnauba wax can be considered to be excellent given that only about of a fourth of leaked oil is fast-leaking. The amount of oil that is fast-leaking in gels made with both RBX and sunflower wax is roughly a third to half of the maximum amount of oil leaked. As such, stability of these gels in both the short- and long-term is similar.

Prior to the discussion, it must be noted that several of the values are derived from other values and as such the correlations will be mirrored along these lines. As an example, Φ_{Fast} and Φ_{Slow} are related by $\Phi_{Slow} = 1 - \Phi_{Fast}$ and as such any variable that exhibits a positive correlation with Φ_{Fast} will exhibit a negative correlation of identical magnitude with Φ_{Slow}. Other values that are related to each other include % Fill and Porosity where Porosity = (100 − % Fill)/100. For the sake of brevity, such near-identical correlations will not be discussed as it is understood that similar trends and mechanisms are operating in these correlations.

Examining the correlations between the microstructural factors and the oil binding parameters (Table 7) obtained from the two-phase exponential fit, it can be seen that the total amount of oil (as a percentage of the available oil) that is leaked does not exhibit a correlation with any of the microstructural parameters. However, the box-counting fractal dimension and the % Fill (the percentage of pixels in a micrograph that is due to solids) show a positive correlation with the percentage of the total exuded oil that is fast-leaking (Φ_{Fast}). The box-counting fractal dimension is a measure of how evenly the mass in the material (as determined by microscopy) is distributed throughout the material (with a higher box-counting fractal dimension indicative of a more even distribution). This correlation suggests that as the mass is more evenly distributed (micrograph is more evenly "covered" by solid mass), the amount of fast-leaking unbound oil as a fraction of the total amount of oil exuded, increases. Likewise, as the volume fraction of solids in the material (determined as the % Fill) increases, so does the percentage of oil that is fast-leaking. Similarly, as the porosity (amount of "void space" that can be occupied by oil which is calculated from the % Fill) of the material increases, the percentage of the total amount of oil that is fast-leaking decreases.

What this suggests is that, as the solid mass is more evenly distributed through the material, the oil present in the material is more strongly bound (a decrease in the percentage of total oil that is slow-leaked and a increase in the percentage of total oil that is fast-leaked). This may sound counter-intuitive but one must recall that if the oil is strongly bound, it may either exude at a very slow rate or it may not exude at all. In the latter case, the oil is so strongly bound that it is not released in the time scale of the experiment and thus the percentage of oil that is fast-leaked out of the total amount that is exuded will actually increase. Indeed, this can be observed in the Y_{Fast} values of 1 % CLX and 2 % CLX, both of which have a high Φ_{Fast}. The Y_{Fast} values of these materials either remain approximately equal to the Y_{Fast} values of other materials or they decrease as in the case of 2 % CLX. Thus, the higher Φ_{Fast} values of these gels are not due to an increase *per se* of the amount of weakly bound oil that is fast-leaked but is rather due to an increase in the amount of oil that is not exuded from the material.

Table 7 Linear correlation analysis of structural and mechanical parameters in the wax crystal network to fit parameters obtained from the fit of the two-phase exponential decay model to the oil-binding data

	D_b	% Fill	Porosity	SFC (%)	G′ (Pa)	Avg. length (mm)	Y_{max} (%)	Y_{Fast} (%)	Y_{Slow} (%)	Φ_{Fast}	Φ_{Slow}	k_{fast}	k_{slow}
D_b						−0.79				0.88	−0.88		−0.80
% Fill						−0.89				0.90	−0.90		−0.86
Porosity						0.89				−0.90	0.90		0.86
SFC (%)								−0.90					
G′ (Pa)								−0.84					
Avg. length (mm)	−0.79	−0.89	0.89							−0.88	0.88	0.92	0.92
Y_{max} (%)													
Y_{Fast} (%)				−0.90	−0.84								
Y_{Slow} (%)													
Φ_{Fast}	0.86	0.90	−0.90			−0.88							
Φ_{Slow}	−0.86	−0.90	0.90			0.88							
k_{fast}						0.92							
k_{slow}	−0.80	−0.86	0.86			0.92							

The reported values are Pearson correlation coefficient (r), indicative of the strength and direction of the correlation. The p values are reported. Given the small number of points available for the correlation, a significance level of $p < 0.2$ is used to judge the merit of whether a correlation warrants discussion or not

As the box-counting fractal dimension, % Fill and Φ_{Fast} show a negative correlation (Table 7) with the average length of the particle, this suggests that as the microstructural elements in a material becomes smaller and smaller, the amount of oil that is more strongly-bound increases such that the oil is not released in the time scale of the experiment. This is reasonable to expect since as the size of the microstructural particles decreases, the total amount of surface area of the solids increases, which increases the amount of oil that is bound by increase the amount of surface that the oil can adsorb to.

There is also a negative correlation between Y_{Fast} and both the % SFC and G′ (Table 7), which suggests that as amount of solids increases, the amount of oil that is bound strongly will also increase and likewise the amount of oil that is weakly bound (out of the total amount of oil in the system) will decrease. This is not unexpected given that as the amount of solids increase, the total surface area that can adsorb oil also increases. The negative correlation between Y_{Fast} and G′ is perhaps is due to the correlation between both of these variables with % SFC. It is well known that G′ is strongly correlated to % SFC in a power law fashion [29]. As such, the higher the % SFC, the higher the G′ and by extension, the higher the amount of oil that is unbound. A direct explanation of this correlation is that the more structured a material is, the lower the amount of oil that is fast-leaking and thus, the better its oil-binding capacity.

There is a negative correlation between both the % Fill and the box-counting fractal dimension and the k_{Fast} and k_{Slow} rate constants (Table 7). What these correlations suggest is that as the solid mass is more evenly distributed through space, the rate at which both the unbound and bound oil exude out of the material is decreased. This is in agreement with the previous discussion that as the box-counting fractal dimension increases, so does the strength of the oil-binding. There is also a positive correlation between the porosity and both the k_{Fast} and k_{Slow} rate constants. This correlation suggests that as the amount of void space within the material increases, so does the rate at which oil is exuded from the material. The last correlation to note is that between the k_{fast} and k_{Slow} rate constants and the average size of the solid particles. This correlation shows that as the size of the solid particles increases, the rate at which the oil leaks out from the material also increases. This is in agreement with previous correlations that show that the degree of oil-binding is much stronger with smaller particles, which presumably have a higher surface area to which oil molecules can be adsorbed onto.

The main conclusion that can be drawn from the following analysis is that gels made with candelilla wax have the highest oil-binding capacity. Likely explanations of this high oil-binding capacity are the small particle size of candelilla wax particles in the gel as well as the homogeneous distribution of these particles throughout the material. RBX and SFX, on the other hand, have relatively larger anisotropic microstructural elements (crystalline fibers) in that one dimension of these microstructures is much larger than the other dimensions. These particles are efficient at gelation but however, form larger void spaces that would result in weaker binding of oil. As well, given that the gels examined are all at their critical concentrations, the microstructure of RBX and sunflower wax ensure efficient gelation compared to candelilla wax and carnauba wax. However, at the critical concentration, RBX and sunflower wax gels will contain less solids and will likewise have a lower surface area that is available to bind oil.

Conclusion

This paper has characterized the microstructure, thermal and mechanical properties as well as the oil-binding capacity of waxes in the neat bulk and gel state, demonstrating that waxes can serve as feasible alternative oil-structuring agents. As demonstrated, the macroscopic properties of these wax oleogels, in particular, the oil-binding capacity, is a direct result of the unique microstructural elements formed by these substances in the gel state. The analysis of oil-binding has elucidated some relationships between the oil-binding stability of these gels and certain microstructural elements, all of which indicate that an even distribution of mass and an increase in the size of the microstructural particles in a gel are correlated with a higher oil-binding capacity.

Work done by other groups has demonstrated that the physiochemical properties of wax oleogels are highly sensitive to both solvent type and the presence of impurities. Changes in the chemical nature of the solvent modify the microstructural morphology, thermal, and rheological properties of these gels. Thus, by extension, the oil-binding properties of the gels are also modified. As such, the presence of minor components, particularly for CLX and CRX, can be regarded as causative of the unique granular microstructural morphology of gels made with these waxes as compared to RBX and SFX.

The small sizes of these microstructural particles lead to their homogenous distribution as characterized by a higher fractal dimension than those of RBX, SFX, and CRX oleogels. The result of small crystals and an even spatial distribution of mass is a material that has superior oil-binding capacities as was observed for gels containing 1 and 2 % (w/w) CLX, due to presumably higher total surface areas for binding oil as well as smaller pores that result in stronger retention of the oil within the material.

Acknowledgments The authors acknowledge the financial support of the Natural Sciences and Engineering Research Council of Canada.

References

1. Health Canada (2014) General questions and answers on trans fats. http://www.hc-sc.gc.ca/fn-an/nutrition/gras-trans-fats/tfa-age_question-eng.php. Accessed 02 Feb 2014
2. American Heart Association (2014) Trans fats (online). http://www.heart.org/HEARTORG/GettingHealthy/FatsAndOils/Fats101/Trans-Fats_UCM_301120_Article.jsp. Accessed 02 Feb 2014
3. Norris S (2007) Trans fats: the health burden. Parliamentary Research and Information Service, Science and Technology Division PRB 05-21E
4. Health Canada (2014) Trans fat monitoring program (Online). http://www.hc-sc.gc.ca/fn-an/nutrition/gras-trans-fats/tfa-age_tc-tm-eng.php. Accessed 02 Feb 2014
5. Marangoni AG (2002) The nature of fractality in fat crystal networks. Trends Food Sci Technol 13:37–47
6. Sato K (2005) Polymorphism in fats and oils. In: Shahidi F (ed) Bailey's industrial oil and fat products, vol 1, 6th edn. Wiley, Hoboken, pp 77–120
7. Le Révérend B, Fryer PJ, Coles S, Bakalis S (2010) A method to qualify and quantify the crystalline state of cocoa butter in industrial chocolate. J Am Oil Chem Soc 87:239–246
8. Marangoni AG, McGauley S (2002) Static crystallization behaviour of cocoa butter and its relationship to network microstructure. In: Marangoni AG, Narine SS (eds) Physical properties of lipids. CRC Press, Boca Raton, pp 85–124
9. Flory PJ (1953) Principles of polymer chemistry. Cornell University Press, Ithaca
10. Marangoni AG, Garti N (2010) Novel strategies for nanostructuring liquid oils into functional fats. In: Marangoni AG, Garti N (eds) Edible oleogels: structure and health implications. AOCS Press, Urbana-Champaign, pp 5–10
11. Dassanayake LSK, Kodali DR, Ueno S, Sato K (2009) Physical properties of rice bran wax in bulk and organogels. J Am Oil Chem Soc 86:1163–1173
12. Toro-Vazquez JF, Morales-Rueda JA, Dibildox-Alvarado E, Charó-Alonso M, Alonzo-Macias M, González-Chávez MM (2007) Thermal and textural properties of organogels developed by candelilla wax in safflower oil. J Am Oil Chem Soc 84:989–1000
13. Hwang HS, Kim S, Singh M, Winkler-Moser JK, Liu SX (2012) Organogel formation of soybean oil with waxes. J Am Oil Chem Soc 89:639–647
14. Rocha JCB, Lopes JD, Mascarenhas MCN, Arellano DB, Guerreiro LMR, da Cunha RL (2013) Thermal and rheological properties of organogels formed by sugarcane or candelilla wax in soybean oil. Food Res Int 50:318–323
15. Food and Agricultural Organization (2013) FAO rice market monitor. XVI(2) (Online). http://www.fao.org/economic/est/publications/rice-publications/rice-market-monitor-rmm/en/. Accessed 02 July 2013
16. Food and Agricultural Organization (2013) Minor oil crops—individual monographs (Noog abyssinia–Nutmeg; Perilla–Pili nut; Rice bran–Sacha inche) (Online). http://www.fao.org/docrep/x5043e/x5043e0a.htm. Accessed 02 July 2013
17. Food and Agricultural Organization (2013) Agribusiness handbook—sunflower crude and refined oils (Online). http://www.responsibleagroinvestment.org/sites/responsibleagroinvestment.org/files/FAO_Agbiz%20handbook_oilseeds_0.pdf. Accessed 02 July 2013
18. Martini S, An MC (2000) Determination of wax concentration in sunflower seed oil. J Am Chem Soc 77:1087–1092
19. Secretaría de Medio Ambiente y Recursos Naturales (2013) Anuarios de la Producción Forestal. http://www.cnf.gob.mx:8080/snif/portal/component/phocadownload/category/23-anuarios-estadisticos?download=151:anuarios-estadisticos-de-la-produccion-forestal-2009. Accessed 02 July 2013
20. Dassanayake LSK, Kodali DR, Ueno S, Sato K (2012) Crystallization kinetics of organogels prepared by rice bran wax and vegetable oil. J Oleo Sci 61:1–9
21. Co E, Marangoni AG (2012) An alternative edible oil-structuring method. J Am Oil Chem Soc 89:749–780
22. Botega DC (2012) Application of rice bran wax organogel to substitute solid fat and enhance unsaturated fat content in ice cream. M.Sc. thesis, Department of Food Science, University of Guelph, Guelph, Canada
23. Toro-Vazquez JF, Alonzo-Macias M, Dibildox-Alvarado E, Charó-Alonso MA (2009) The effect of tripalmitin crystallization on the thermomechanical properties of candelilla wax organogels. Food Biophys 9:199–212
24. Smith KW, Bhaggan K, Talbot G, van Malssen KF (2011) Crystallization of fats—influence of minor components and additives. J Am Oil Chem Soc 88:1085–1101
25. Wright A, Marangoni AG (2002) Effect of DAG on milk fat TAG crystallization. J Am Oil Chem Soc 79:395–402
26. Kerr RM, Tombokan X, Ghosh S, Martini S (2011) Crystallization behaviour of anhydrous milk fat—sunflower oil wax blends. J Agric Food Chem 59:2689–2695
27. Narine SS, Marangoni AG (1999) Relating structure of fat crystal networks to mechanical properties: a review. Food Res Int 32:227–248
28. Marangoni AG, Tang D (2006) Microstructure and fractal analysis of fat crystal networks. J Am Oil Chem Soc 83:377–388
29. Narine SS, Marangoni AG (1999) Fractal nature of fat crystal networks. Phys Rev E 59:1908–1920